Microwave plasma chemical vapor deposition of nano-composite C/Pt thin-films

Marek Marcinek, Xiangyun Song, Robert Kostecki *

Environmental Energy Technologies Division, Lawrence Berkeley National Laboratory, Berkeley, CA 94720, USA

Abstract

Composite carbon–platinum thin-films of nano-crystalline graphitic carbon decorated with uniformly-dispersed 2–4 nm Pt nano-particles have been synthesized from a solid organic precursor by a one-step microwave plasma chemical vapor deposition (MPCVD). The fast Ar-plasma discharge and the presence of microwave radiation accelerate the formation of sites suitable for *in situ* heterogeneous nucleation, and consequently, the fine dispersion of metal in the carbonaceous matrix. The electrochemical response of the 2 μm C/Pt thin-film electrode displays electrochemical activity, which is attributed to the high ca. 18 m^2/g effective surface area of Pt nano-particles.
© 2007 Elsevier B.V. All rights reserved.

Keywords: C/Pt; Catalyst; Plasma; Microwave

1. Introduction

The ability to prepare well-dispersed, high surface area electrocatalysts has significantly increased the viability of many electrochemical processes. The introduction of carbon black-supported platinum catalysts has helped lower the platinum loading in proton exchange membrane fuel cell (PEMFC) electrodes from several mg$_{Pt}$/cm^2 to less than 0.2 mg$_{Pt}$/cm^2, with no detrimental effect on the fuel cell performance [1]. The development of high surface area, porous carbon supports suitable for composite catalysts has been the subject of considerable interest in recent years [2–7]. The carbon matrix provides mechanical support and electronic continuity, enables uniform dispersion, and inhibits the agglomeration of catalyst nano-particles. It also offers suitable channels for gas and ion transport and exhibits good corrosion resistance [8].

Synthesis of highly-dispersed, supported Pt/C nano-particles with uniform size and morphology still remains a challenge for high-performance catalysts. Conventional deposition techniques of nano-sized Pt catalyst particles at carbonaceous substrates are mostly based on ion exchange [9], wet impregnation [10,11], chemical or electrochemical precipitation [12,13], and colloidal techniques [14–16]. However, these techniques provide only limited control of particle size and morphology.

Plasma application to produce membrane–electrode assemblies (MEAs) with ultra-low catalyst loading for applications in miniature fuel cells was reported by Mex et al. [17–19]. Microwave-generated hydrogen plasma was used as a reducing agent to precipitate Pt nano-particles from aqueous solutions of H$_2$PtCl$_6$ [20,21]. Microwave radiation was also applied for rapid heating of solutions of dissolved metal salts to promote the nucleation and accelerate growth of metal clusters [22–27].

High-power microwave plasma chemical vapor deposition (MPVCD) reactors have been widely used to prepare thin-films of patterned carbon nano-tubes [28–30] and diamond [31–33]. The MPVCD synthesis of amorphous, sp^2-coordinated carbon thin-films [34], carbon fibers [35], and nano-crystalline graphite (NCG) [36,37] have also been reported.

* Corresponding author.
 E-mail address: r_kostecki@lbl.gov (R. Kostecki).

In this work we present a novel, one-step MPVCD synthesis of a composite NCG/Pt catalyst thin-film. We demonstrate a simple, fast, and inexpensive method for the simultaneous formation of an electronically conductive carbon support decorated with uniformly distributed ultra-fine Pt catalyst that can be deposited on any type of substrate without the use of stabilizers or reducing agents.

2. Experimental

Fig. 1 shows a diagram of the two-segment Pyrex glass tube reactor (5 cm internal diameter, 17 cm long) and a schematic representation of the deposition process. Each cylindrical segment was fitted with a vacuum valve. One end of the reactor was connected to a two-stage mechanical vacuum pump whereas the other end was hooked up to an argon supply manifold. The reactor was held tightly together by a rubber clamp (not shown) and sealed with an O-ring fitted between the segment collars.

A small amount ($\sim$2 mg) of the platinum (II) acetyl-acetonate ($Pt(C_5H_7O_2)_2$) (Sigma–Aldrich) organic precursor powder was positioned at one end of a glass slide whereas a $0.5\ cm^2$ piece of highly-oriented, pyrolitic graphite (HOPG) or glass substrate was positioned $\sim$5 mm away from the precursor at the other end of the glass slide. The reactor was purged with Ar for 90 s with a flow of $2\ dm^3/min$, evacuated to 1.2×10^{-1} Torr, and positioned in close vicinity to a 2.45 GHz, 1200 W magnetron. The geometry of the system was designed to generate Ar plasma in the reactor with the hot edge of the plasma region near the organic precursor source and the cool edge of the plasma glow near the substrate. The MPACVD reactor was enclosed in a nitrogen-filled glove box to eliminate any possible interference from oxygen impurities.

The onset of microwave radiation led to an instantaneous Ar-plasma discharge in the reactor and fast evaporation of the Pt-acetyl-acetonate through the dipolar polarization heating mechanism. A typical MPCVD process was continued for 20 s and produced a $\sim$2 μm thick nano-composite C/Pt film on the substrate. The C/Pt film composition was reproducible for the given organic precursor and deposition time. The qualitative analysis of the C/Pt films by the direct current plasma emission spectroscopy and combustion infrared detection produced a C/Pt mass ratio of 1:3, i.e., much lower than in the platinum (II) acetyl-acetonate (5:8). The observed carbon loss is associated mainly with the decomposition of carboxyl groups and formation of CO and CO_2.

The structure of carbon in composite C/Pt films was analyzed by Raman microscopy (Labram, ISA Group Horiba with laser excitation wavelength 632.8 and 488 nm, 10 mW), transmission electron microscopy (TEM, model JEOL 200CX), and scanning electron microscopy (SEM, model Hitachi S-4300 SE/N).

Cyclic voltammetry experiments were conducted at room temperature in a single-compartment, three-electrode cell filled with $0.5\ M\ H_2SO_4$ deaerated aqueous solution with a model 273A Princeton Applied Research potentiostat/galvanostat. A Pt mesh and $Hg/Hg_2Cl_2/KCl$ (sat) were used as counter and reference electrodes, respectively.

3. Results and discussion

Fig. 2 shows the typical average Raman microscopy spectra of a C/Pt thin-film recorded at 632.8 and 488 nm excitation wavelengths. Each spectrum consists of two broad peaks which originate from sp^2-hybridized graphitic and amorphous carbons. The so-called G-band at $1582\ cm^{-1}$ and D-band at $\sim 1323\ cm^{-1}$ ($\lambda = 632$ nm) or $1344\ cm^{-1}$ ($\lambda = 488$ nm) correspond to the E_{2g} and A_{1g} mode of graphite, respectively [38]. The origin of the
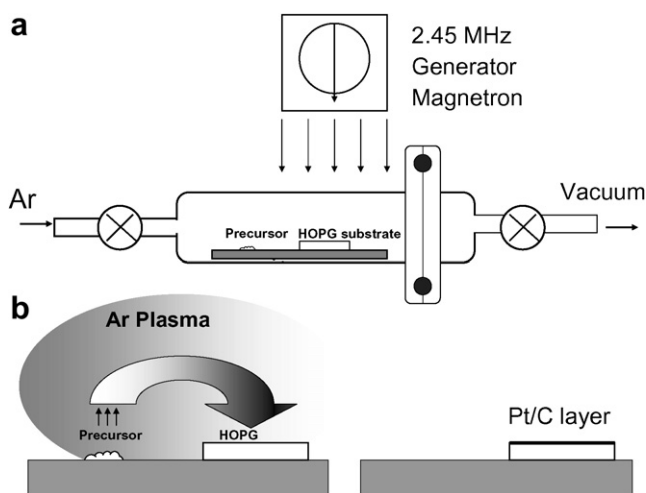

Fig. 1. A diagram of the microwave plasma chemical vapor deposition system (a) and schematic representation of the deposition of C/Pt thin-films (b).
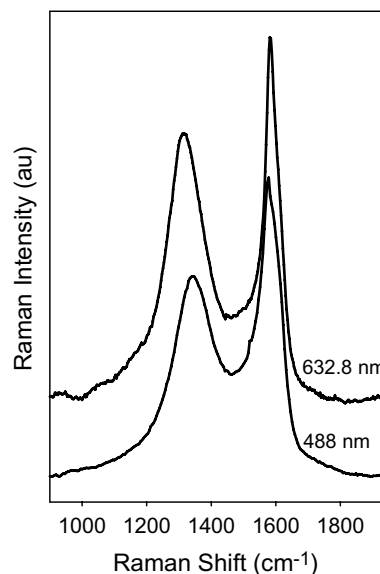

Fig. 2. Multi-wavelength micro-Raman spectra of MPCVD C/Pt composite films, using excitation wavelength of 632.8 and 488 nm.

D-band is associated with the breakage of symmetry that occurs at the edges of graphite sheets and point defects. An additional shoulder at $1620 \, cm^{-1}$ (D′-band) is also attributed to discontinuity and disorder within graphene planes but its exact origin is still under debate [39].

As the excitation wavelength is varied, different carbon structures resonate at different energies. The presence of strong graphite G and D modes, along with the absence of a sharp diamond Raman peak at $\sim 1330 \, cm^{-1}$, suggest that the carbon films consist mainly of a sp^2-coordinated carbon phase. The location of the G-band of graphite and carbon blacks is quite insensitive to the excitation wavelength. However, the observed shift of the D-band location from 1323 to $1344 \, cm^{-1}$ and the decreased peak intensity as the laser excitation is varied from 632.8 to 488 nm are typical of nano-crystalline graphite with a high degree of order [36,40].

Fig. 3a and b depicts scanning electron micrographs of a cross-section and surface morphology of the C/Pt composite film. The SEM images display a continuous thin surface film of fairly uniform thickness ca. 2 μm. The morphology of the film is very porous and consistent in the film bulk and at the surface. The film consists of large ~ 300–600 nm, featureless agglomerates, which are fused together into a micro- and nano-porous "lava rock"-like structure.

The EDX spectrum and surface elemental map of platinum are shown in Fig. 3c and d, respectively. Strong carbon (0.27 keV) and platinum (2.06 keV) peaks as well as the absence of an oxygen peak at 0.53 keV suggest a complete decomposition of the organic precursor in the Ar plasma. The EDX Pt map reveals a uniform distribution of fine platinum particles in the composite C/Pt film. The X-ray diffraction pattern of the C/Pt layer (not shown here) displays broad peaks characteristic of face-centered cubic (fcc) Pt. The average Pt particle size calculated from the Scherrer equation was ~ 4 nm.

Fig. 4a and b shows bright- and dark-field TEM images of C/Pt agglomerates. The images show a remarkably uniform and fine dispersion of platinum in the C/Pt composite. The HRTEM image (Fig. 4c) reveals a few 2–4 nm Pt particles that are embedded in partially graphitized, carbonaceous material. Interestingly, the carbon adjacent to the platinum particles shows well-organized graphene planes, whereas the bulk of the carbon displays shorter layers of irregular shape, which are typical of carbon blacks. The Pt particle size distribution was obtained by directly measuring the size of 300 randomly-chosen particles in the magnified TEM images. The particle size distribution is very narrow (Fig. 4d). The calculated average size of Pt particles (ca. 2.7 nm) is noticeably smaller than the average particle size estimated from the X-ray data.

The C/Pt thin-film produced by MPCVD on HOPG substrate was characterized by cyclic voltammetry (CV) in an aqueous solution of 0.5 M H_2SO_4 (Fig. 5). The potential was scanned between -0.28 and 1.29 V (vs. SCE) at a rate of 50 mV/s. The peaks for hydrogen and oxygen
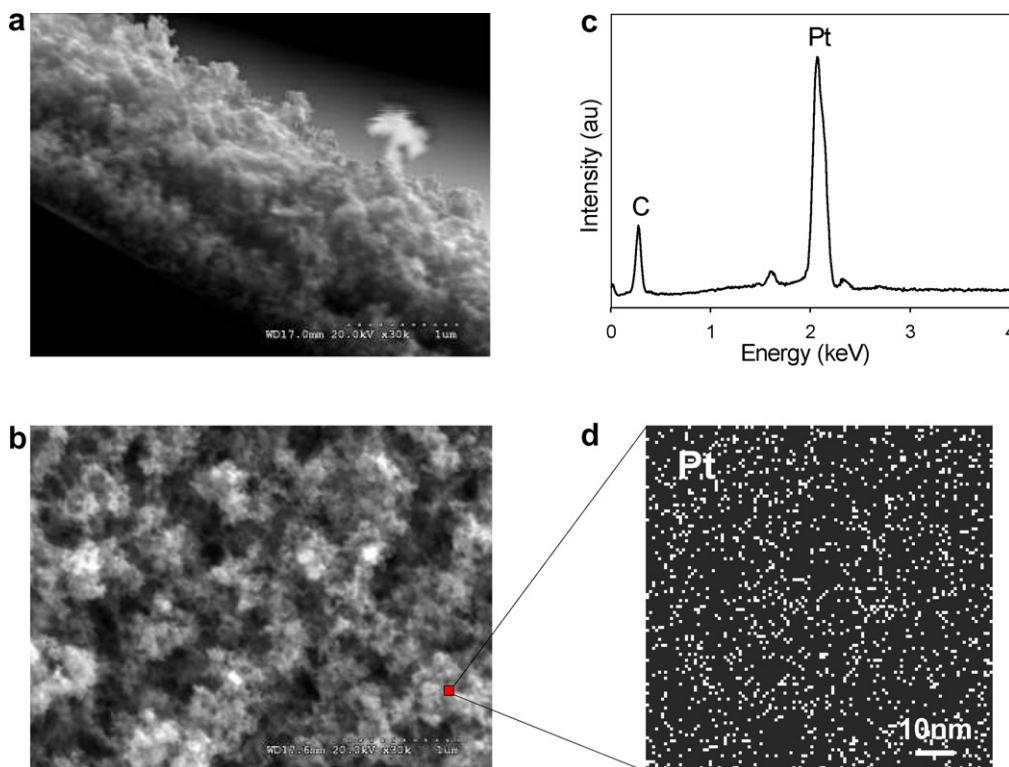

Fig. 3. SEM micrographs of cross-section (a), surface (b), the corresponding EDX spectrum (c), and surface elemental map of platinum (d) of the C/Pt composite film deposited on glass for 20 s, using platinum (II) acetyl-acetonate.
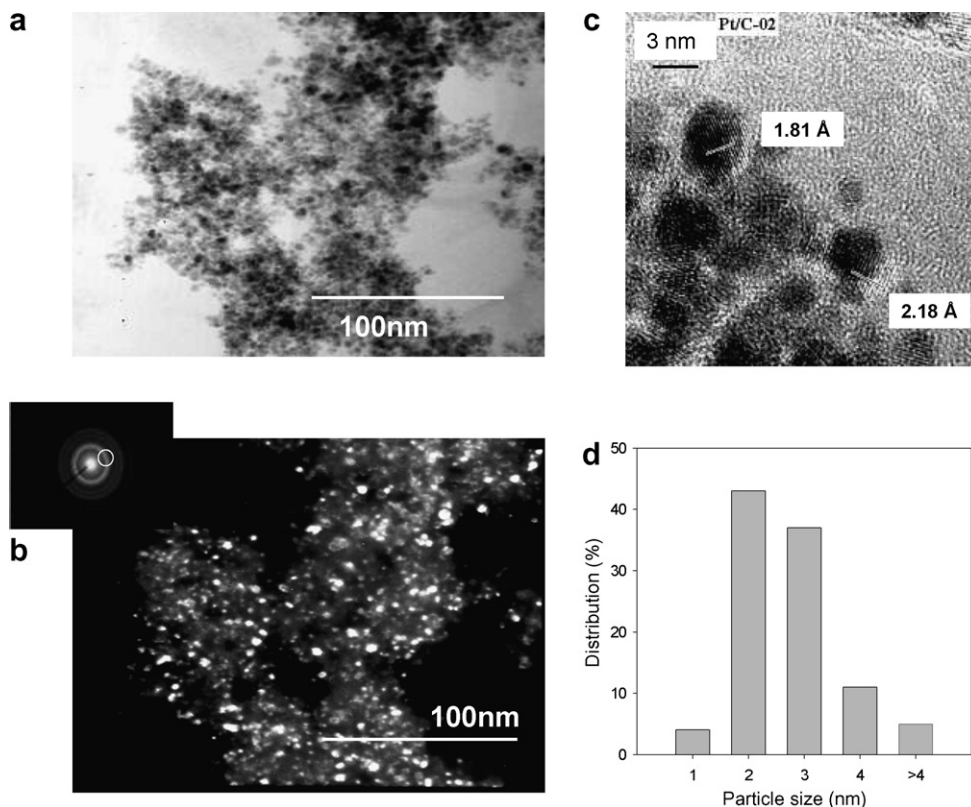
Fig. 4. Bright-field (a) and dark-field (b) TEM images of C/Pt composite particles deposited by MPCVD. (c) HRTEM image of Pt particles embedded in carbonaceous matrix. (d) Pt particle size distribution in the C/Pt composite.
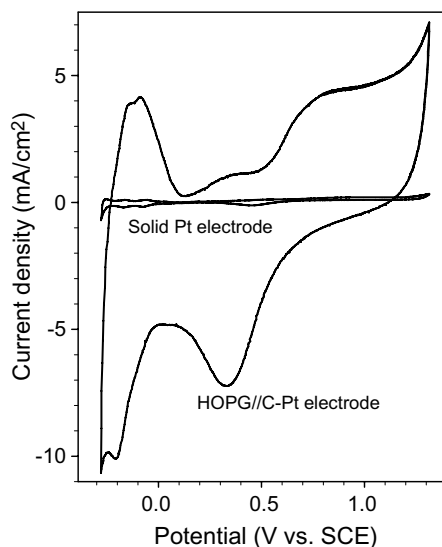

Fig. 5. Cyclic voltammograms of the C/Pt composite film produced by MPCVD on a HOPG substrate, and a solid Pt electrode. The measurements were carried out in 0.5 M H_2SO_4 with a scan rate 50 mV/s at room temperature.

adsorption–desorption, characteristic of polycrystalline Pt, are clearly visible and are in agreement with the literature data [41]. The real surface area of the platinum catalyst could be estimated from the ratio of the integrated charge of the hydrogen adsorption peaks of the Pt polycrystalline

and C/Pt composite electrodes, assuming that dispersed Pt retains its bulk properties. The effective surface area of the C/Pt thin-film electrode is ∼60 times larger per geometric area unit than the polycrystalline Pt, which yields a Pt catalyst active surface area ca. 18 m^2/g.

4. Conclusions

In summary, MPVCD co-synthesis of a nano-structured C/Pt composite thin-film described in this study presents a simple, fast, and inexpensive method for the one-step formation of electronically-conductive, carbon/metal composite catalyst beds, which can be deposited on any type of substrate. The microwave-assisted co-deposition of platinum and carbon had evidently facilitated the nucleation and growth of small and uniform Pt particles in a nanocrystalline carbon matrix. The fast plasma discharge and the presence of microwave radiation accelerate the formation of sites suitable for *in situ* heterogeneous nucleation, and consequently, the fine dispersion of metal in the carbonaceous matrix. The electrochemical response of the C/Pt thin-film electrode displays electrochemical activity, which is attributed to the high surface area Pt nano-particles.

References

[1] T.R. Ralph, M.P. Hogarth, Platinum Met. Rev. 46 (2002) 3.

[2] J.B. Goodenough, A. Hamnett, J.B. Kennedy, R. Manoharan, S.A. Weeks, J. Electroanal. Chem. 240 (1990) 133.

[3] J.M. Planeix, N. Coustel, B. Coq, V. Brotons, P.S. Kumbhar, R. Duatartre, P. Ganeste, P. Bernier, P.M. Ajayan, J. Am. Chem. Soc. 116 (1994) 7935.

[4] M. Uchida, Y. Fukuoka, Y. Sugawara, N. Eda, A. Ohta, J. Electrochem. Soc. 143 (1996) 2245.

[5] S.H. Joo, S.J. Choi, M. Oh, J. Kwak, Z. Liu, O. Terasaki, R. Ryoo, Nature 412 (2001) 169.

[6] Z. Hou, B. Yi, H. Zhang, Electrochem. Solid-State Lett. 6 (2003) A232.

[7] V. Raghuveer, A. Mantiram, J. Electrochem. Soc. 152 (2005) A1504.

[8] N. Staud, H. Sokol, P.N. Ross Jr., J. Electrochem. Soc. 136 (1989) 3570.

[9] R. Yu, L. Chen, Q. Liu, J. Lin, K.L. Tan, S.C. Ng, H.S.O. Chan, G.Q. Xu, T.S.A. Hor, Chem. Mater. 10 (1998) 718.

[10] G.L. Che, B.B. Lakshmi, E.R. Fisher, C.R. Martin, Nature 393 (1998) 346.

[11] B. Rajesh, K.R. Thampi, J.M. Bonard, N. Xanthopoulos, H.J. Mathieu, B. Viswanathan, J. Phys. Chem. B 107 (2003) 2701.

[12] B.C. Satishkumar, E.M. Vogl, A. Govindaraj, C.N.R. Rao, J. Phys. D 29 (1996) 3173.

[13] Z.L. Liu, X.H. Lin, J.Y. Lee, W. Zhang, M. Han, L.M. Gan, Langmuir 18 (2002) 4054.

[14] T. Fujimoto, A. Fukuoka, S. Iijima, M. Ichikawa, J. Phys. Chem. 97 (1993) 279.

[15] S.A. Lee, K.W. Park, J.H. Choi, B.K. Kwon, Y.E. Sung, J. Electrochem. Soc. 149 (2002) A1299.

[16] X. Li, S. Ge, C.L. Hui, I.M. Hsing, Electrochem. Solid-State Lett. 7 (2004) A286.

[17] L. Mex, J. Muller, Membr. Technol. 115 (1999) 5.

[18] L. Mex, N. Ponath, J. Muller, Fuel Cells Bull. 39 (2001) 9.

[19] L. Mex, M. Sussiek, J. Muller, Chem. Eng. Commun. 190 (2003) 1085.

[20] I.G. Koo, M.S. Lee, J.H. Shim, J.H. Ahn, W.M. Lee, J. Mater. Chem. 15 (2005) 4125.

[21] K.Y. Joung, J.H. Shim, I.G. Koo, M.S. Lee, W.M. Lee, in: 208th Electrochem. Soc. Meeting, Los Angeles, October 16–21, 2005, Abstract #29.

[22] Z. Liu, X.Y. Ling, J.Y. Lee, X. Su, L.M. Gan, J. Mater. Chem. 13 (2003) 3049.

[23] S. Komoarneni, D. Li, B. Newalkar, H. Katsuki, A.S. Bhalla, Langmuir 18 (2002) 5959.

[24] Z. Liu, X.Y. Ling, J.Y. Lee, J. Phys. Chem. B 108 (2004) 8234.

[25] W.X. Tu, H.F. Liu, Chem. Mater. 12 (2000) 564.

[26] W.X. Chen, J.Y. Lee, J.L. Liu, Chem. Commun. 21 (2002) 2588.

[27] Z.L. Liu, J.Y. Lee, W.X. Chen, M. Han, L.M. Gan, Langmuir 20 (2004) 181.

[28] O.M. Kuttel, O. Groening, L. Schlapbach, Appl. Phys. Lett. 73 (1998) 2113.

[29] H. Murakami, M. Hirakawa, C. Tanaka, H. Yamakawa, Appl. Phys. Lett. 76 (2000) 1776.

[30] J.I.B. Wilson, N. Scheerbaum, S. Karim, N. Polwart, P. John, Y. Fan, A.G. Fitzgerald, Diamond Relat. Mater. 11 (2002) 918.

[31] V.G. Ralchenko, A.A. Smolin, V.I. Konov, K.F. Sergeichev, I.A. Sychov, I.I. Vlasov, V.V. Migulin, S.V. Voronina, A.V. Khomich, Diamond Relat. Mater. 6 (1997) 417.

[32] T.P. Mollart, K.L. Lewis, Diamond Relat. Mater. 8 (1999) 236.

[33] C.J. Tang, A.J. Neves, M.C. Carmo, J. Phys.: Condens. Matter 17 (2005) 1687.

[34] Y. Lifshitz, C.H. Lee, Y. Wu, W.J. Zhang, I. Bello, S.T. Lee, Appl. Phys. Lett. 88 (2006) 243114.

[35] J. Zou, X. Zeng, X. Xiong, H. Tang, L. Li, Q. Liu, Z. Li, Carbon 45 (2007) 828.

[36] R.C. Mani, M.K. Sunkara, R.P. Baldwin, J. Gullapalli, J.A. Chaney, G. Bhimarasetti, J.M. Cowley, A.M. Rao, R. Raod, J. Electrochem. Soc. 152 (2005) E154.

[37] M. Marcinek, R. Kostecki, in: 208th Electrochem. Soc. Meeting, Los Angeles, October 16–21, 2005, Abstract #114.

[38] F. Tunistra, J.L. Koenig, J. Chem. Phys. 53 (1970) 1126.

[39] R. Saito, A. Jorio, A.G. Souza Filho, G. Dresselhaus, M.S. Dresselhaus, M.A. Pimenta, Phys. Rev. Lett. 88 (2002) 027401.

[40] A.D. Lueking, H.R. Gutierrez, D.A. Fonseca, E. Dickey, Carbon 45 (2007) 751, and references therein.

[41] K.W. Park, J.H. Choi, B.K. Kwon, S.A. Lee, Y.E. Sung, H.Y. Ha, S.A. Hong, H. Kim, A. Wieckowski, J. Phys. Chem. B 106 (2002) 1869, and references therein.